Nucleophilic attack at the central allyl carbon atom in [(.eta.3-allyl)ML2]+ complexes (M = palladium, platinum). Experimental facts and new theoretical insights

Carla Carfagna, Roberta Galarini, Klaus Linn, Jose A. Lopez, Carlo Mealli, and Alfredo Musco

Organometallics, **1993**, 12 (8), 3019-3028• DOI: 10.1021/om00032a026 • Publication Date (Web): 01 May 2002

Nucleophilic Attack at the Central Allyl Carbon Atom in $[(\eta^3\text{-allyl})ML_2]^+$ Complexes (M = Pd, Pt). Experimental Facts and New Theoretical Insights

Carla Carfagna,† Roberta Galarini,† Klaus Linn,‡ José A. López,‡ Carlo Mealli,*,‡ and Alfredo Musco*,†

Istituto di Scienze Chimiche, Università degli Studi di Urbino, 61029 Urbino, Italy, and Istituto per lo Studio della Stereochimica ed Energetica dei Composti di Coordinazione (ISSECC, CNR), Via J. Nardi 39, 50132 Firenze, Italy

Received January 8, 1993

The reaction of ketene silyl acetals with $[(\eta^3\text{-allyl})PtL_2]^+OAc^-$ leads to formation of platina(II)cyclobutanes upon the nucleophilic attack of the enolate at the central allyl carbon atom (C_c). As a result, from a new theoretical analysis for complexes of the type $[(\eta^3\text{-allyl})ML_2]^+$ (M = Pd, Pt), the C_c-centered MO (C_3-$\pi_\perp$*) is not destabilized as usually assumed. Rather, it competes with another MO, (d_π-nC_3) (centered on metal and terminal C_t carbon atoms), to be the first LUMO of the system. On this basis, the attack of a nucleophile at the C_c atom is almost as probable as attack at the C_t atoms. The initial MO picture of the precursor complex can only suggest the regioselectivity of the reaction, saying nothing about the attractive/repulsive interactions encountered by the incoming nucleophile in the pathway toward metallacyclobutane. Within the limits imposed by the EHMO method, a simple qualitative description is offered of the intended correlations among metal–carbon and carbon–nucleophile bonding/antibonding MO's during the formation of the metallacyclobutane product. An energetic barrier, which varies as a function of the σ-donor strength of the nucleophile, is observed, and its origin is described.

Introduction

The attack of carbon nucleophiles at the terminal allyl carbon atom (C_t) in palladium complexes is considered a powerful synthetic method for carbon–carbon bond formation. The nature of the nucleophile is known to play a crucial role. For instance, nonstabilized carbanions appear to react preferentially on the metal side, whereas stabilized carbanions attack directly one C_t atom of the coordinated allyl group.[1] The nucleophilic attack for analogous platinum complexes is less documented, but in light of the available data, it appears to follow similar trends.[2]

At present, there is increasing evidence that, similar to the case for some Mo, W, Rh, and Ir allyl species,[3] also Pd complexes of the type $[(\eta^3\text{-allyl})PdL_2]^+$ (L = phosphine ligand) may be attacked at the central carbon atom (C_c). This fact was first reported by Hegedus[4] and then by some of us,[5] who have carried out the reaction of ketene silyl acetals 1 with allylic acetates in the presence of Pd phosphine complexes. The final attainment of cyclopropanes suggests that the initial formation of an unstable palladacyclobutane intermediate is followed by reductive elimination. The simultaneous formation of large quantities of allyl alkylation products indicates that the attacks at either C_t or C_c atoms are competitive; therefore, the regioselectivity is low (eq 1).

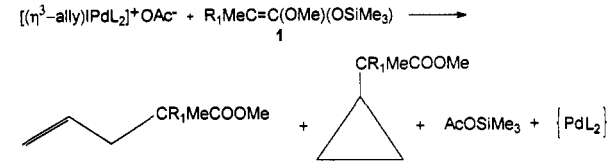

(1)

A preliminary extension of the palladium chemistry to platinum proved to be fruitful, as it showed that the reaction of $[(\eta^3\text{-allyl})PtL_2]^+$ with 1 proceeds with remarkable regioselectivity at the C_c atom to yield stable platinacyclobutane complexes.[6] Surprisingly, the regioselectivity observed with $[(\eta^3\text{-allyl})ML_2]^+$ (M = Pd, Pt; L = phosphine) is switched in the presence of nitrogen chelating ligands. Thus, stoichiometric[7] as well as catalytic reactions,[8] if one starts from $[(\eta^3\text{-allyl})Pd(TMEDA)]^+$ (TMEDA = *N,N,N',N'*-tetramethylethanediamine), yield cyclopropanes. In contrast, the analogous (TMEDA)Pt complex yields mainly allylation products. Here we present in detail the synthesis and the spectroscopic characterization of the platina(II)cyclobutane complexes

† Università degli Studi di Urbino.
‡ ISSECC, CNR.

(1) Trost, B. M.; Verhover, T. R. In *Comprehensive Organometallic Chemistry*; Wilkinson, G., Stone, F. G. A., Abel, E. W., Eds.; Pergamon Press: Oxford, U.K., 1982; Vol. 8, p 799.

(2) (a) Kurosawa, H. *J. Chem. Soc., Dalton Trans.* **1979**, 939. (b) Brown, J. M.; MacIntyre, J. E. *J. Chem. Soc., Perkin Trans. 2* **1985**, 961.

(3) (a) Mo, W.; Ephritikhine, M.; Francis, B. R.; Green, M. L. H.; MacKenzie, R. E.; Smith, M. J. *J. Chem. Soc., Dalton Trans.* **1977**, 1131. Ephritikhine, M.; Green, M. L. H.; MacKenzie, R. E. *J. Chem. Soc., Chem. Commun.* **1976**, 619. (b) Rh, Ir: McGhee, W. D.; Bergman, R. G. *J. Am. Chem. Soc.* **1985**, *107*, 3388. Periana, R. A.; Bergman, R. G. *J. Am. Chem. Soc.* **1986**, *108*, 7346. Tjaden, E. B.; Stryker, J. M. *J. Am. Chem. Soc.* **1990**, *112*, 6420. Tjaden, E. B.; Stryker, J. M. *Organometallics* **1992**, *11*, 16. Wakefield, J. B.; Stryker, J. M. *J. Am. Chem. Soc.* **1991**, *113*, 7057.

(4) Hegedus, L. S.; Darlington, W. H.; Russel, C. E. *J. Org. Chem.* **1980**, *45*, 5193.

(5) (a) Carfagna, C.; Mariani, L.; Musco, A.; Sallese, G.; Santi, R. *J. Org. Chem.* **1991**, *56*, 3924. (b) Carfagna, C.; Galarini, R.; Musco, A.; Santi, R. *J. Mol. Catal.* **1992**, *72*, 19.

(6) Carfagna, C.; Galarini, R.; Musco, A.; Santi, R. *Organometallics* **1991**, *10*, 3956.

(7) Hoffmann, H. M. R.; Otte, A. R.; Wilde, A. *Angew. Chem., Int. Ed. Engl.* **1992**, *31*, 234.

(8) Formica, M.; Musco, A.; Pontellini, R.; Linn, K.; Mealli, C. *J. Organomet. Chem.* **1993**, *448*, C6.

0276-7333/93/2312-3019$04.00/0

Table I. Relevant ^1H and ^{31}P NMR Data[a] for

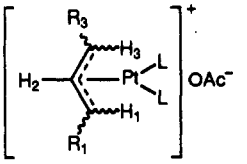

			chem shift (δ) and coupling constant (Hz)						
complex[b]	R_1	R_3	$H_{1,syn}$	$H_{1,anti}$	$H_{3,syn}$	$H_{3,anti}$	H_2	others	^{31}P
3a	H	H	4.45 ($^3J_{HH}$ = 7.3, J_{HP} = 5)	3.14 ($^3J_{HH}$ = 13.3, J_{HP} = 8, J_{HPt} = 30)			4.7		38.6 (J_{PPt} = 4343)
3b[c]	H	H	3.80 (J_{HH} = 6.4)	2.93 ($^3J_{HH}$ = 12.7, J_{HP} = 7, J_{HPt} = 40)			5.53		16.7 (J_{PPt} = 3950)
5c[d]	Me	H		3.67 ($^3J_{HH}$ = 13, J_{HP} = 8)	3.13[b]	2.79 ($^3J_{HH}$ = 13, J_{HP} = 9)	5.2	1.23 (Me)	20.2 (J_{PPt} = 3840)
									17.5 (J_{PPt} = 4123)
5e[d,e]	Me	H	4.34		4.02	2.5	5.4	1.02 (Me)	17.9 (J_{PPt} = 4011)
									15.9 (J_{PPt} = 3824)
5f[d]	Me	Me	3.89 ($^3J_{HH}$ = 8)			3.36 ($^3J_{HH}$ = 12.7, J_{HP} = 9)	5.22	1.1 (Me_{anti})	19.0 (J_{PPt} = 3806)
								1.4 (Me_{syn})	17.7 (J_{PPt} = 4094)
5d[d,e]	Me	Me		3.58			4.70 ($^3J_{HH}$ = 12)	1.0 (Me)	20.4 (J_{PPt} = 4033)

[a] In $CDCl_3$. [b] **3a**, L = PCy_3; **3b**, **5c–f**, L = PPh_3; stereochemistry of complexes **5** as indicated in Scheme I. [c] –20 °C. [d] –50 °C. [e] Missing J values due to either overlapping or low-intensity signals.

obtained from the reaction of **1** with (η^3-allyl)Pt complexes. Also, since this type of chemistry is intriguing from a theoretical viewpoint, notwithstanding previous efforts,[9] a new MO analysis of the factors affecting nucleophilic attack at $[(\eta^3\text{-allyl})ML_2]^+$ complexes is presented.

Results

Experimental Facts. Preparation of the Complexes. $((allyl)PtCl)_4$[10] (**2**) is a convenient starting material for the preparation of platina(II)cyclobutane complexes. The reaction procedure is outlined in eqs 2 and 3. Addition of stoichiometric amounts of the appropriate phosphorus ligand to a methylene chloride suspension of **2** yields a solution of $[(\eta^3\text{-allyl})PtL_2]^+Cl^-$ which readily reacts with TlOAc to yield $[(\eta^3\text{-allyl})PtL_2]^+Ac^-$ (**3**).

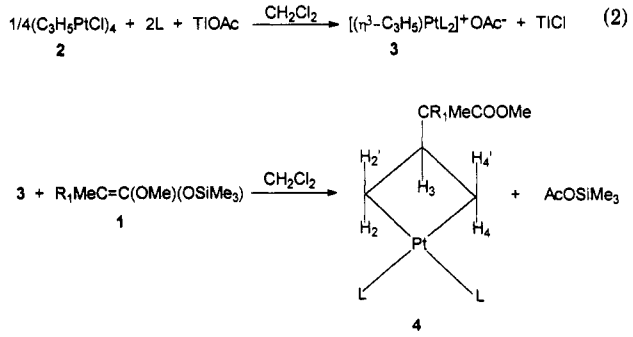

4a R_1 = Me; L = $P(C_6H_{11})_3$
4b R_1 = Me; L = PPh_3
4c R_1 = Me; L-L = $PPh_2(CH_2)_4PPh_2$
4d R_1 = H; L-L = $PPh_2(CH_2)_4PPh_2$
4e R_1 = Me; L-L = $PPh_2(CH_2)_2PPh_2$

(3)

Subsequent addition of **1** yields platina(II)cyclobutane complexes which are readily isolated from the reaction mixture. Evaporation of the solvent after elimination of TlCl, followed by washing of the residue with methanol, yields complexes **4** as white, air-stable, solid materials. The reaction method outlined in eqs 2 and 3 allows preparation of β-substituted platina(II)cyclobutane complexes with a variety of coordinated phosphorus ligands.

A reaction method which implies no limitation on the substitution of the ring carbon atoms is reported in eq 4.

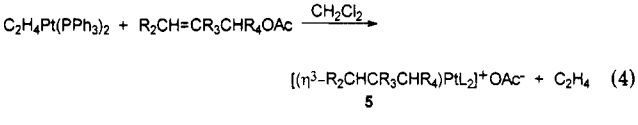

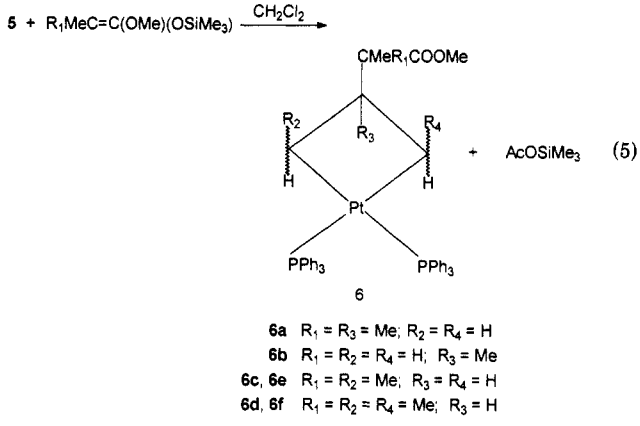

6a $R_1 = R_3$ = Me; $R_2 = R_4$ = H
6b $R_1 = R_2 = R_4$ = H; R_3 = Me
6c, 6e $R_1 = R_2$ = Me; $R_3 = R_4$ = H
6d, 6f $R_1 = R_2 = R_4$ = Me; R_3 = H

Addition of the appropriate allylic acetate to $C_2H_4Pt(PPh_3)_2$ in methylene chloride yields the corresponding allyl acetate complex **5**, which reacts with **1** to yield the platina(II)cyclobutane complexes **6**. Both of the above reaction methods produce platina(II)cyclobutane complexes in good yields (see Experimental Section). The ^1H and ^{31}P NMR spectroscopic characterization of some representative (allyl)Pt acetate complexes in $CDCl_3$ clearly indicates that the allyl group is η^3 bonded to platinum (Table I). At room temperature, in all cases except for $[(\eta^3\text{-allyl})Pt(PCy_3)_2]^+OAc^-$ (**3a**), broad resonances indicated the presence of dynamic processes such as η^3–η^1 equilibrium and ligand exchange. At lower temperatures

(9) (a) Sakaki, S.; Nishikawa, M.; Ohyoshi, A. *J. Am. Chem. Soc.* **1980**, *102*, 4062. (b) Davies, S. G.; Green, M. L. H.; Mingos, D. M. P. *Tetrahedron* **1978**, *34*, 3047; *Nouv. J. Chem.* **1977**, *1*, 445. (c) Curtis, M. D.; Eisenstein, O.; *Organometallics* **1984**, *3*, 882.
(10) Lukas, J. *Inorg. Synth.* **1974**, 15.

Table II. Relevant NMR Data[a] for

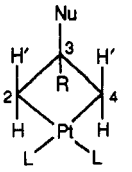

compd	L	chem shift (δ) and coupling constant (Hz)					
		H_2', H_4'	H_2, H_4	R	C_2, C_4	C_3	^{31}P
4a (R = H)	PCy_3	−0.01 (J_{HPt} = 78)	0.66 (J_{HPt} = 70)	2.84	−10.2 (J_{CP} = 82, J_{CPt} = 430)	51.2 (J_{CPt} = 128)	23.0 (J_{PPt} = 1882)
4b (R = H)	PPh_3	0.10 (J_{HPt} = 84)	0.44 (J_{HPt} = 80)	3.02	−7.3 (J_{CP} = 80, J_{CPt} = 413)	50.8 (J_{CPt} = 128)	25.9 (J_{PPt} = 1902)
4c (R = H)	DPPB	0.06 (J_{HPt} = 82)	0.58	3.08	−9.8 (J_{CP} = 81, J_{CPt} = 402)	51.3 (J_{CPt} = 136)	16.0 (J_{PPt} = 1872)
4d (R = H)	DPPB	−0.20, −0.04 (J_{HPt} = 81)	0.74, 0.74 (J_{HPt} = 78)	3.04	−8.7, −7.1 (J_{CP} = 83, J_{CPt} = 398)	47.4 (J_{CPt} = 139)	15.9 (J_{PPt} = 1861) 16.0 (J_{PPt} = 1842)
4e (R = H)	DPPE	0.72 (J_{HPt} = 81)	1.55 (J_{HPt} = 78)	3.36	−10.2 (J_{CP} = 88, J_{CPt} = 405)	52.1 (J_{CPt} = 144)	42.5 (J_{PPt} = 1799)
6a (R = Me)	PPh_3	0.56 (J_{HPt} = 83)	0.11 (J_{HPt} = 83)	1.01	1.5 (J_{CP} = 79, J_{CPt} = 415)	50.3 (J_{CPt} = 116)	26.5 (J_{PPt} = 1895)
6b (R = Me)	PPh_3	0.1–0.7[b]	0.1–0.7[b]	0.97	4.0, 4.4 (J_{CP} = 79, 78, J_{CPt} = 412, 408)	47.3 (J_{CPt} = 122)	26.1 (J_{PPt} = 1870) 26.6 (J_{PPt} = 1903)

[a] In $CDCl_3$. [b] Signals of ring protons overlap.

Table III. Relevant NMR Data[a] for

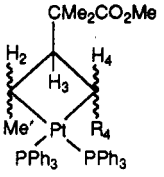

com-plex[b]	chem shift (δ) and coupling constant (Hz)								
	H_2	H_4	R_4	Me'	H_3	C_2	C_4	C_3	^{31}P
6c	0.60	0.00 (J_{HPt} = 90)	0.34 (J_{HPt} = 80)	0.75 ($^3J_{HH}$ = 7.0)	3.06	−2.8 (J_{CP} = 85, J_{CPt} = 459)	−10.3 (J_{CP} = 76, J_{CPt} = 420)	60.0 (J_{CPt} = 12, 8)	24.3 (J_{PPt} = 1610) 25.8 (J_{PPt} = 1985)
6e[c]				0.8		9.9 (J_{CP} = 80)	−6.8 (J_{CP} = 76)	53.7	21.7 (J_{PPt} = 1640) 28.4 (J_{PPt} = 2093)
6f	1.33 ($J_{H_2H_3}$ = 7)	1.04 ($J_{H_4H_3}$ = 9)	0.80–0.90	0.80–0.90	3.24	3.7, 8.8 (J_{CP} = 85, 77, J_{CPt} = 508, 472)	3.7, 8.8 (J_{CP} = 85, 77, J_{CPt} = 508, 472	60.9 (J_{CPt} = 12, 2)	22.9 (J_{PPt} = 1771) 26.6 (J_{PPt} = 1820)
6d[c]				0.65 ($^3J_{HH}$ = 7.0, J_{HP} = 9)		−6.3 (J_{CP} = 81, J_{CPt} = 460)		69.2 (J_{CPt} = 12, 8)	24.3 (J_{PPt} = 1668)

[a] In $CDCl_3$. [b] Stereochemistry of complexes **6** as indicated in Scheme I. [c] Resonances which are not reported overlap with signals of the major isomer.

resonances of the static η^3 structures were observed. The ^1H and ^{31}P NMR spectra of $[(\eta^3\text{-allyl})Pt(PPh_3)_2]^+Ac^-$ (**3b**) and $[(\eta^3\text{-1-methylallyl})Pt(PPh_3)_2]^+OAc^-$ (**5c**(*syn*):**5e**(*anti*) = 3:1) have the same chemical shifts and J values as $[(\eta^3\text{-allyl})Pt(PPh_3)_2]^+BF_4^-$ [11] and $[(\eta^3\text{-1-methylallyl})Pt(PPh_3)_2]^+X^-$ (X^- = BF_4^-, Cl^-; *syn*:*anti* = 3:1),[2b,12] respectively; thus, the acetate group is not coordinated. On the other hand, $[(\eta^3\text{-allyl})Pt(PCy_3)_2]^+OAc^-$ (**3a**) and $[(\eta^3\text{-allyl})Pt(PCy_3)_2]^+BF_4^-$ (**8**) have significantly different chemical shifts in $CDCl_3$ at room temperature.[12] Therefore, **3a** might be more properly described as an ion pair. It is noteworthy that the allyl group of (allyl)PtL_2X (X = halide) has been reported as η^3 and η^1 bonded in polar and apolar solvents, respectively.[11,13] As chloroform and methylene chloride have comparable polarities, the η^3 coordination, observed in $CDCl_3$, should also be retained in methylene chloride, which is the solvent of choice for the coupling reaction. The role played by the acetate group is essential, as it assists the nucleophilic attack of the silyl enolate by activating the Si–O bond of **1**.[14]

Ketone silyl enolates appear to be less reactive than ketene silyl acetals. Silyl enolates **7** and **9** do not react with **3**, but reaction with $[(\eta^3\text{-}C_3H_5)Pt(PPh_3)_2]^+Cl^-$ in methylene chloride in the presence of $Bu_4N^+F^-$ produced the expected platina(II)cyclobutane complexes **8** and **10**, respectively (eqs 6 and 7). Activation of a Si–O bond by F^- has been exploited in several silyl enolate reactions with electrophiles.[15]

Complexes **4**, **6**, **8**, and **10** have been characterized by NMR spectroscopy (Tables II and III). In all cases peculiar upfield resonances were observed in the ^1H and ^{13}C NMR

(11) Boag, N. M.; Green, M.; Spencer, J. L.; Stone, F. G. A. *J. Chem. Soc., Dalton Trans.* **1980**, 1208.

(12) **8**: ^{31}P NMR (δ, $CDCl_3$) 28.2 (J_{PtP} = 3786 Hz); ^1H NMR (δ, $CDCl_3$) 5.00 ($H_{central}$), 4.92 (H_{syn}, J_{HH} = 6.2 Hz), 2.51 (H_{anti}, J_{HH} = 12.4 Hz, J_{HP} = 8.0 Hz, $J_{HPt} \simeq$ 41 Hz). See also: Attig, T. G.; Clark, H. C. *J. Organomet. Chem.* **1975**, *94*, C49.

(13) Kurosawa, H.; Yoshida, G. *J. Organomet. Chem.* **1976**, *120*, 297.

(14) Hertler, W. R.; Rajanbabu, T. V.; Ovenall, D. W.; Reddy, G. S.; Sogah, D. Y. *J. Am. Chem. Soc.* **1988**, *110*, 5841.

(15) Chuit, C.; Corriu, R. J. P.; Reyè, C. *J. Organomet. Chem.* **1988**, *358*, 57 and references quoted therein.

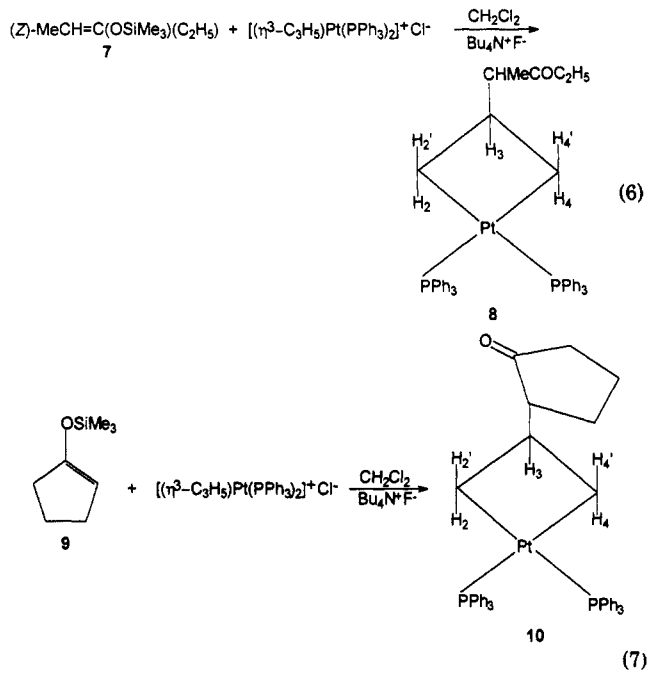

spectra assignable to α-hydrogens and -carbons. Similar observations have been made by other authors.[3,16,17] The stereochemistry of complexes **6c–f** has been elucidated by NOE experiments and has been confirmed by observing upfield shifts of the pertinent ^{13}C signals due to γ-substituent effect.[18]

Stereochemistry of the Reaction. Reaction of the probe substrate **11** with **1** in the presence of Pd complexes yielded moderate quantities of cyclopropane **12** and the allylated product **13**. The stereochemistry of **12** is consistent with an external attack of the silyl enolate **1** (eq 8).[5a]

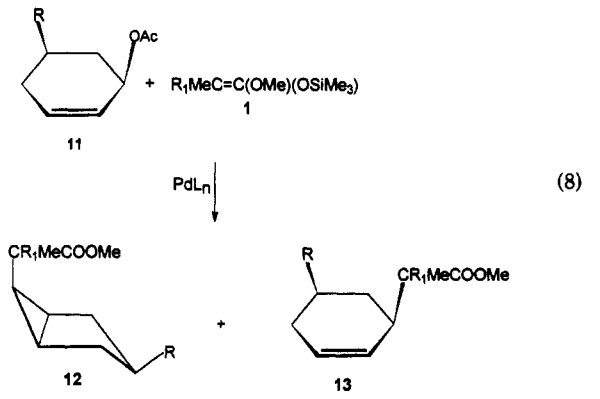

Disappointingly, reaction of **11** with $C_2H_4Pt(PPh_3)_2$ and then with **1** (R = Me) produced exclusively the allylated product **13**. However, the stereochemistry of the products isolated from the reaction of **1** (R_1 = Me) with $[(\eta^3$-1-methylallyl)$Pt(PPh_3)_2]^+OAc^-$ and $[(\eta^3$-1,3-dimethylallyl)$Pt(PPh_2)_2]^+OAc^-$, respectively, is consistent with an external attack of the silyl enolate (Scheme I).

According to ^1H and ^{31}P NMR spectra, $[(\eta^3$-1-methylallyl)$Pt(PPh_3)_2]^+OAc^-$ exists as a 3:1 mixture of

Scheme I

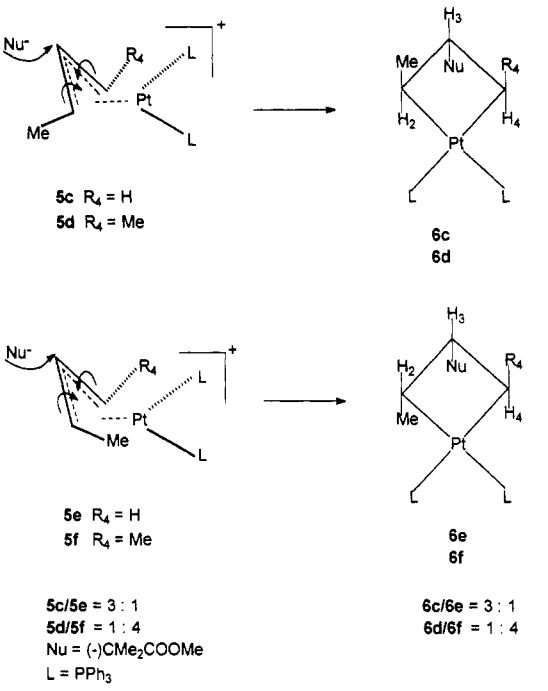

syn (**5c**) and *anti* (**5e**) isomers and $[(\eta^3$-1,3-dimethylallyl)$Pt(PPh_3)_2]^+OAc^-$ as a 4:1 mixture of *syn,anti* (**5f**) and *syn,syn* (**5d**) isomers (Table I). Platina(II)cyclobutanes **6c,e** and **6d,f**, which are derived from the 1-methylallyl and 1,3-dimethylallyl complexes, respectively, have been isolated in the same isomeric ratio as above. Therefore, the isomeric ratio of the platina(II)cyclobutanes parallels that of the corresponding allyl complexes. Thus, upon external attack of the enolate on the C_c atom, the complexes **6c,d** are formed from $[(syn$-1-methylallyl$)Pt(PPh_3)_2]^+OAc^-$ (**5c**) and $[(syn,syn$-1,3-dimethylallyl$)Pd(PPh_3)_2]^+OAc^-$ (**5d**), respectively. Analogously, complexes **6e,f** are formed from **5e,f**. A disrotatory motion around the allylic carbon–carbon bonds accounts for the overall stereochemistry of the platinacyclobutane ring. Within the ring, the *trans* or the *cis* placement of the α-carbon substituent, with respect to the β-carbon substituent, corresponds to the *syn* and the *anti* geometry of the terminal allyl carbon atoms, respectively.

In one case, the reversibility of the attack of the nucleophile on the central allyl carbon atom was observed. A $CDCl_3$ solution of isomers **6f,d** decomposes slowly. The ^1H NMR spectrum of a solution kept for 3 days in the dark and at room temperature showed the signals of olefin **15**, methyl isobutyrate (**16**), and methyl 2-deuterio-2-methylpropanoate (**17**) (Scheme II), unchanged **6d**, and low-intensity unassignable peaks.

The ^{31}P NMR spectrum, with trimethyl phosphate as the internal standard, confirmed that compound **6f** disappeared to yield unidentified Pt species while the concentration of **6d** did not change. These experimental results may be rationalized by assuming that the enolate dissociates from **6f** either to attack regiospecifically the resulting η^3-allyl cation **5f** on the carbon atom bearing the anti methyl group to yield the intermediate Pt(0) complex **14** or to abstract either hydrogen or deuterium from the reaction medium to yield **16** and **17**, respectively.[19]

(16) Klinger, R. J.; Huffman, J. C.; Kochi, J. K. *J. Am. Chem. Soc.* **1982**, *104*, 2147.
(17) Foley, P.; DiCosimo, R.; Whitesides, G. M. *J. Am. Chem. Soc.* **1980**, *102*, 6713.
(18) Breitmaier, E.; Voelter, W. *Carbon-13 NMR Spectroscopy*; VCH: New York.

(19) **15–17** have been identified by GLC and ^1H NMR comparison with authentic samples.

Scheme II

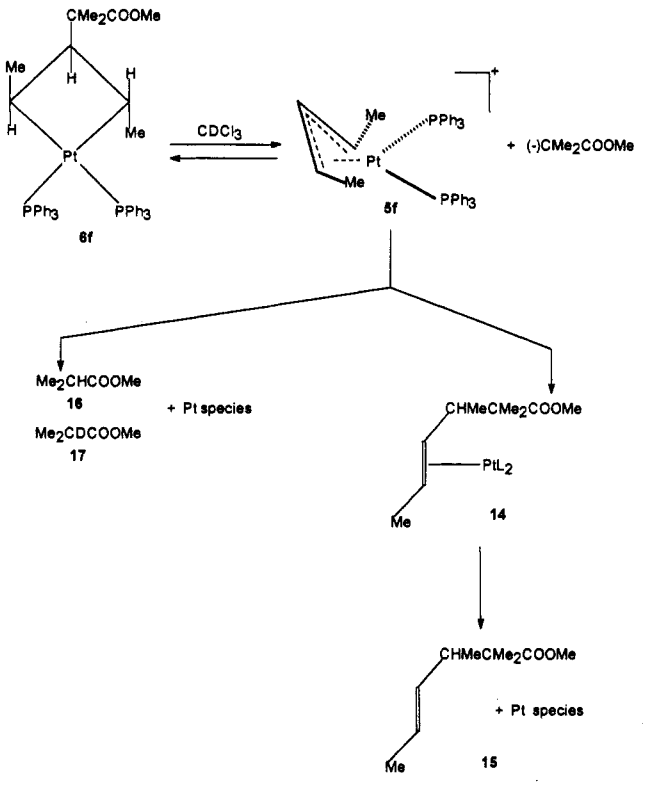

Reversibility of nucleophilic addition at the central allyl carbon of $[(C_5Me_5)(Me_3P)M(\eta^3\text{-allyl})]^+$ (M = Rh, Ir) has been previously observed by Tjaden and Stryker.[3b]

Theoretical Analysis. General Aspects. Upon the attack of selected nucleophiles at $[(\eta^3\text{-allyl})ML_2]^+$ complexes, the formation of metallacyclobutanes is competitive with that of olefins. In view of the new experimental evidence, the electronic factors governing the site of the attack have been reexamined also by considering the results of previous theoretical analyses.[9]

Recall that the allyl $\pi_\perp$ system is subdivided into three fragment molecular orbitals (FMO's), of which I can donate electron density to an empty metal σ hybrid. The out-of-phase combination of p_π orbitals on the C_t atoms (the so-called nonbonding pair *n*, II) interacts with a suitable metal d_π level. Finally, the allyl's FMO $C_3\text{-}\pi_\perp^*$ (see III) is little involved in interactions with the metal, also because it is more centered on the C_c atom that lies out of the main $L_2M(C_t)_2$ coordination plane.

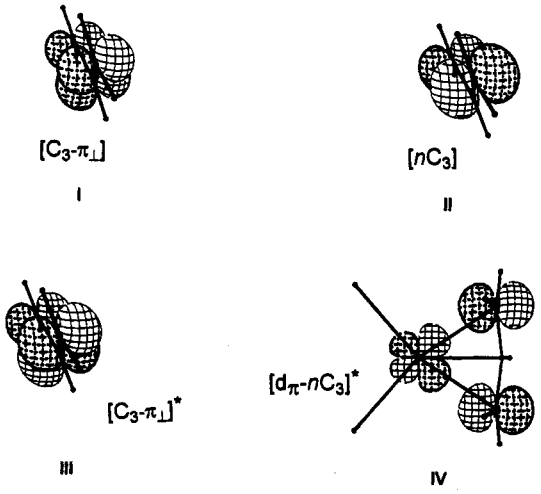

It is generally accepted that, due to its overall $C_3\text{-}\pi_\perp^*$ character, III lies well above the antibonding combination $[d_\pi\text{-}nC_3]^*$ (IV, first LUMO). Also, since IV receives a large contribution from the C_t atoms, the formation of olefin adducts upon nucleophilic attack seems sequential.

Curtis and Eisenstein[9c] explored whether different transition-metal fragments may invert the order of the two empty MO's (III and IV) and hence promote a different regioselectivity for the nucleophilic attack. Indeed, these authors found that the fragment Cp_2Mo has a metal d_π frontier hybrid apt to destabilize $[d_\pi\text{-}nC_3]^*$ over $C_3\text{-}\pi_\perp^*$. This agrees well with the formation of metallacyclobutanes upon the attack of an hydride at $(\eta^3$-allyl)$MoCp_2$ complexes, one of the few examples of such a reactivity for the time being.[3a,4] In contrast, the same reactivity seemed generally precluded to $[(\eta^3\text{-allyl})ML_2]^+$ species. Other authors considered the regioselectivity of the nucleophilic attack as being largely *charge controlled*.[9a,b] If a L_nM^+ fragment accepts a sufficient electron density from the anionic allyl ligand, attack at an impoverished C_t atom is predicted. The stronger the d_π/nC_3 interaction that subtracts electrons from $C_3H_5^-$, the higher the antibonding MO $[d_\pi\text{-}nC_3]^*$. However, just for the latter reason attack at the C_c atom seems easier.

The extended Hückel method[20] can still provide at least a good qualitative picture of systems as complex as the present one. It is important, however, that the geometry of the model used is not too *idealized*. In particular, the loss of planarity of the C_3H_5 grouping upon η^3 coordination plays a specific role and it cannot be overlooked.

The feature is evidenced by the crystal structures of complexes containing allyls with substituents bulkier than the hydrogen atoms.[21] In addition, a neutron diffraction study of $Ni(\eta^3\text{-}C_3H_5)_2$ (V) performed by Krüger *et al.*[22] revealed that the five allyl H atoms are significantly off the C_3 plane. In the next section the *ideal* and the *experimental* $(\eta^3$-allyl)M models will be compared.

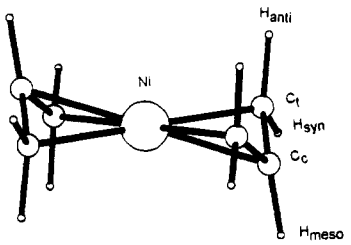

V

Geometric Parametrization of $(\eta^3$-allyl)M Complexes. The MO Picture and Its Implications for Reactivity. In all of the $(\eta^3$-allyl)M complexes the θ angle defined in VI is close to 110°. The inclination of the C_3 plane with respect to the $M(C_t)_2$ plane imposes three equal M–C distances (given a fixed C_t–C_c–C_t angle of 120°). For an overall planar allyl group, the *anti* substituents of the allyl (H_a atoms in VI) are already too close to the metal and four-electron repulsions with filled d orbitals are active.

(20) Hoffmann, R. *J. Chem. Phys.* **1963**, *39*, 1397. Hoffmann, R.; Lipscomb, W. N. *J. Chem. Phys.* **1962**, *36*, 2179. Hoffmann, R.; Lipscomb, W. N. *J. Chem. Phys.* **1962**, *36*, 2872.

(21) Maitlis, P. M.; Espinet, P.; Russell, M. J. H. In *Comprehensive Organometallic Chemistry*; Wilkinson, G., Stone, F. G. A., Abel, E. W., Eds.; Pergamon Press: Oxford, U.K., 1982; Vol. 6, p 385 and references therein.

(22) Goddard, R.; Krüger, C.; Mark, F.; Stansfield, R.; Zhang, X. *Organometallics* **1985**, *4*, 285.

Thus, steric as well as electronic effects (*vide infra*) cause the C_3H_5 grouping to distort from planarity on η^3 coordination.

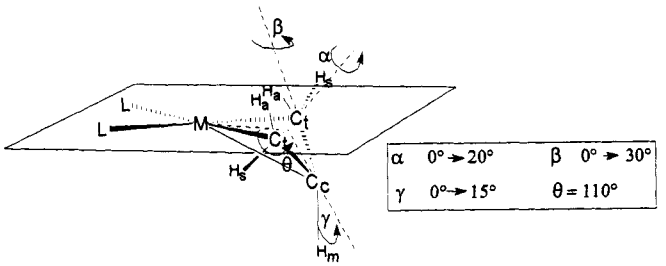

VI

The neutron diffraction study of bis(allyl)nickel (**V**)[22] has shown that the C_t–H_a vectors (*anti*) deviate ca. 30° from the C_3 plane (away from the metal), whereas the C_t–H_s (*syn*) and C_t–H_m (*meso*) vectors are pinned toward the metal by ca. 9 and 16°, respectively. Interestingly, Krüger *et al.* backed their experimental findings with a consistent optimization of the geometry by using *ab initio* methods.[22]

Now, we find it most convenient to express the displacements of the H atoms in terms of the relative orientations of the C_tH_2 planes as well as of the C_cH_m vector with respect to the plane C_3. Such a parametrization smoothly converts an *ideal* model (with planar C_3H_5) into that of the actual (η^3-allyl)M structure. In other words, the *experimental* model is affected by incipient *disrotatory*-like movement of the C_tH_2 groups. In detail, two combined rotations (α and β in **VI**) need to be operated on each C_tH_2 group (θ is fixed at 110°). The α rotation is about an axis in the C_3 plane, which passes through C_t and is perpendicular to the C_c–C_t bond (final α value 20°). The β rotation is about the C_c–C_t bond and must follow the α rotation (β, up to 30°). Finally, the C_c–H_m vector is tilted toward the metal up to an angle (γ) of 15°. With the help of the Walsh diagram of Figure 1, it is now possible to highlight the electronic factors that force the allyl group to lose planarity upon η^3 coordination to a metal fragment.

Consistent with the results for bis(allyl)nickel,[21] the total energy gained at the *experimental* structure (right side of the diagram) is rather large (ca. 1 eV). This is a consequence of the progressive loss of parallelism between the three carbon p_π orbitals forming the original $\pi_\perp$ system. In particular, upon reorientation of the C_tH_2 groups, the allyl's FMO nC_3 (**II**) overlaps better with the lobes of the metal d_π hybrid and the corresponding bonding MO, [d_π-nC_3] at low energy, is significantly stabilized. By analogy, the MO [d_π-nC_3]* is destabilized (compare the reorientation of the C_t p orbitals in **IV** and **VII**, respectively).

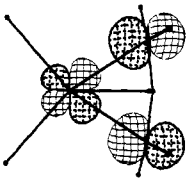

VII

A good part of the total energy gain at the *experimental structure* is due to the latter enhanced interactions.

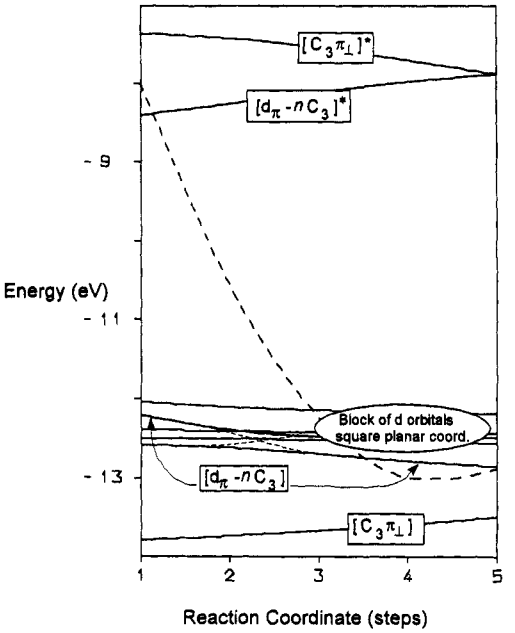

Figure 1. Walsh diagram for the conversion of an *ideal* model of the complex [(η^3-allyl)M(PH_3)$_2$]$^+$ (overall planar allyl group) into the *experimental* one (hydrogen atoms displaced out of the C_3 plane as in the structure of bis(allyl)nickel).[22] The angular parameters are those defined in **VI**. The dashed line shows the total energy variation. A different scale applies to the latter, as each step on the vertical axis is now equal to 0.2 eV.

Additional stabilization of the *experimental* structure comes from the 15° bending of the C_c–H_{meso} vector which reorients the p_π orbital at the C_c atom in the C_3-$\pi_\perp$ bonding combination **I** and thus increases its interaction with the empty metal σ hybrid.

The loss of parallelism among C_3 p_π orbitals does also reduce the overall C_3 antibonding character of the second LUMO (in the *ideal* structure), namely C_3-$\pi_\perp$* (a comparison of the drawing **VIII** with **III** highlights the

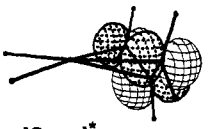

VIII

reorentation of the p orbital of C_c with respect to those of the C_t atoms). Even if C_3-$\pi_\perp$* may potentially become the first LUMO of the system, the gap between [d_π-nC_3]* and C_3 $\pi_\perp$* remains small and, in any case, the precise order of the two LUMOs cannot be reliably established at the EHMO level. Importantly, however, the trend leaves little doubt that a nucleophilic attack becomes almost equally probable at either the C_c or the C_t atoms.

A stabilized C_3 $\pi_\perp$* level, consequent to the allyl's deformation, appears to be a general result for the allyl η^3-coordination. In particular, the known propensity of (η^3-allyl)MCp_2 complexes to undergo nucleophilic attack at the C_c atom is now definitely out of the discussion, as in that case even a planar C_3H_5 grouping confines C_3-$\pi_\perp$* below the MO [d_π-nC_3]*. In the present [(η^3-allyl)ML_2]$^+$ complexes, the closeness of two LUMO's does not allow us to solve *a priori* the dichotomy of the reactivity, but, at variance with some previous theoretical ideas, the

possible nucleophilic attack at the C_c atom is not out of the orbital control.

In principle, the initial regioselectivity can be subtly ruled by discriminants such as the nature of the metal, of the complex substrate, and of the incoming nucleophile. Besides, the possible barriers encountered by the system during the course of the reaction (*vide infra*) may or may not allow the reaction to proceed. Smaller barriers for the nucleophilic addition to the C_c atom would be consistent with the idea, stressed by some authors,[3] that kinetic factors have greater relevance than the thermodynamic ones. Even though one may suspect that the final release of cyclopropanes from the formed metallacyclobutanes is a leading factor for the reactivity of the present system, the EHMO method does not allow us to make reliable quantitative comparisons between the energetic balance of the alternative products. On the other hand, it is possible and chemically significant to detect energy barriers along the pathways and to attempt their qualitative understanding.

In general, a simulation of the least-motion pathways leading to either the olefin or the metallacyclobutane adducts requires the definition of a large number of geometric variables. Whereas the modeling of the reaction leading to olefins imposes the definition of as many as 10 different geometrical parameters[22] and the loss of any symmetry, the modeling of the pathway to metallacyclobutane is simpler (only five variables); moreover, a mirror plane is preserved. More than the energetics from the EHMO calculations, the intended correlations and the graphics of the evolving MO's provide useful chemical information.

Reaction Pathway of the Nucleophilic Attack at the C_c Atom. The same angular parameters defined in **VI** can be further used to attain a planar metallacyclobutane skeleton. At this point, α, β, and γ as well as θ have reached the values 30, 90, 55, and 180°, respectively: An additional reaction coordinate is required to describe the motion of the incoming nucleophile, namely the relative distance C_c–Nu (=d) (see **IX**).

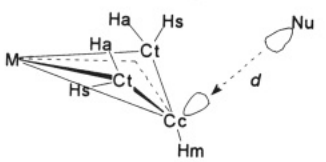

IX

Noteworthily, the proposed reaction pathway, characterized by a nucleophile attacking C_c from the side opposite to the preexisting M–C_c linkage, is fully consistent with the experimental findings reported in a previous section. Recall, in fact (Scheme I), that upon nucleophilic attack at allyls with selected substituents (*syn* or *anti*) the isomeric ratios of the derived platinacyclobutanes (*cis* or *trans*, respectively) remain unchanged. In no case does the breaking of any M–C_t linkage appear to occur.

The need for at least five different parameters to mimic a reaction pathway is a nontrivial modeling task. If all of the parameters in **VI** and **IX** are concertedly varied, the problem becomes monodimensional. Otherwise, the group of the angular parameters (**VI**) can be varied independently from the movement of the nucleophile (distance d in **IX**). The potential energy surface in Figure 2 is relative to the attack of a weak σ-donor (soft nucleophile), in this case

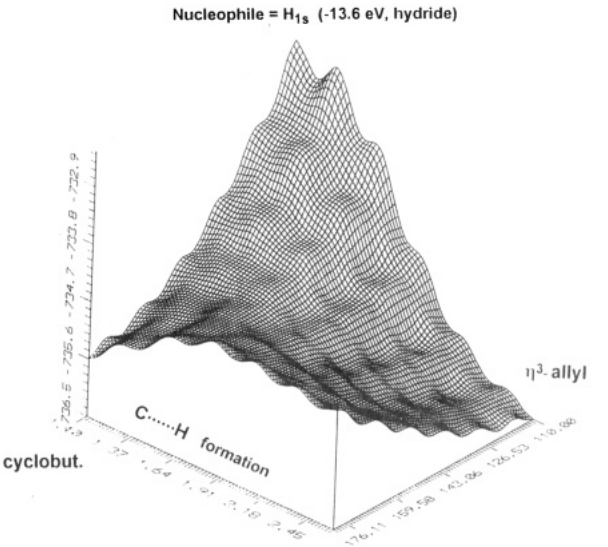

Figure 2. Energy surface for the attack of a nucleophile on a $[(\eta^3\text{-allyl})M(PH_3)_2]^+$ complex to give a metallacyclobutane adduct. The nucleophile is a hydride donor with the standard energy for the H_{1s} orbital (=−13.6 eV).

a hydride anion (the standard energy of the doubly populated H_{1s} orbital is −13.6 eV). The most significant feature is the presence of an energy barrier of at least 1.8 eV. Also, the separated reagents (η^3-allyl complex and nucleophile) are somewhat more stable than the metallacyclobutane product but, as mentioned, we dare not derive any conclusion from this. Other surfaces have been calculated for an increasing donor capabilities of the attacking nucleophile (the electronegativity of the hydride is decreased by changing artificially the energy of H_{1s}). The barrier is progressively flattened and eventually vanishes. Also, the final metallacyclobutane adduct becomes more stable. To highlight the underlying MO effects, we consider only the rearrangement of the η^3-allyl complex to the metallacyclobutane skeleton and exclude the incoming nucleophile, temporarily.

Now, the trends already illustrated in the transformation from the *ideal* to the *experimental* structure are magnified. In particular, the level C_3-$\pi_\perp$* continues to decrease in energy (by ca. 2 eV) because the carbon p_π orbitals become progressively less parallel than in **VIII**. In **X**, the former

X **XI**

C_3-$\pi_\perp$* level is shown to have a lobe properly hybridized to receive a σ-donor electrophile. However, the smooth interaction between the empty and filled orbitals is made more difficult by the presence of the former C_3-$\pi_\perp$ bonding orbital (**I**). This latter MO is also affected by the loss of p_π parallellism and rises in energy. Eventually, upon mixing with a pure d orbital, the former C_3-$\pi_\perp$ character is shared by two filled MO's (in-phase/out-of-phase d_{metal}/C_3-$\pi_\perp$ combinations), one of which is the HOMO, **XI**. Importantly, the two latter levels both have a lobe that points toward the incoming nucleophile so that a net repulsion is predictable. Indeed, just this σ-type repulsion is at the origin of the energetic barrier along the pathway.

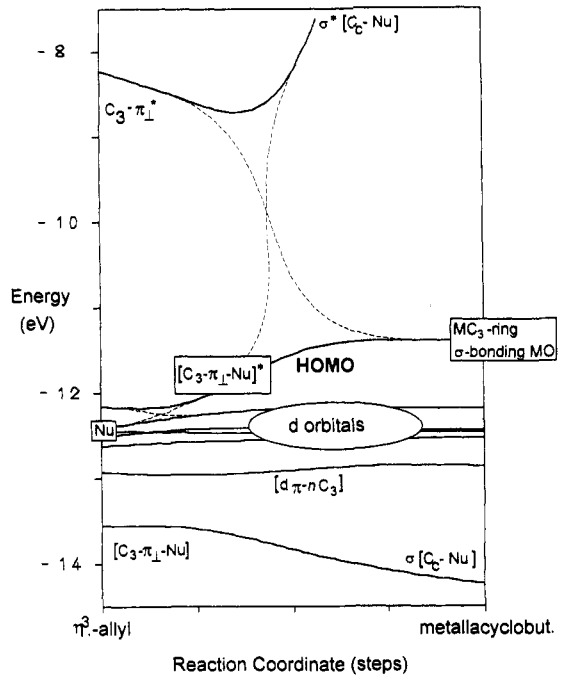

Figure 3. Walsh diagram for the evolution of the frontier MO's along a least-motion pathway that transforms the complex $[(\eta^3\text{-allyl})M(PH_3)_2]^+$ into a metallacyclobutane adduct upon the attack of a nucleophile. The latter is simulated by a pseudo-hydride anion with the energy of the H_{1s} orbital set at −12.5 eV.

Evidently, the *orbital control* of the reaction depends on the relative energies and overlaps of three levels, namely C_3-$\pi_\perp$, C_3-$\pi_\perp$*, and the nucleophile's σ hybrid. Thus, a weak nucleophile (*e.g.* a hydride or a largely stabilized carbanion such as malonate with σ-hybrid energies of −13.6 and *ca.* −12.4 eV, respectively) matches, at some stage of the ring flattening, the energy of the raising C_3-$\pi_\perp$ MO (or of its split partners). The repulsion may not be sufficiently counterbalanced by the attraction with the empty level C_3-$\pi_\perp$*, and eventually, the attack of the nucleophile can be redirected toward one terminal C_t atom. Noteworthily, we have found no trace of a similar type of repulsion along the explored pathways from the η^3-allyl complex toward the olefin product.[23]

When the energy of the nucleophile's σ hybrid is relatively high, there is a clear-cut trend for reducing and eventually eliminating the barrier. In fact, over a certain point the attraction between the nucleophile's and the evolving C_3-$\pi_\perp$* orbitals prevails and the attack at the C_c atom seems to proceed smoothly. Significantly, our experimental data prove that this becomes possible for carboanions which are only slightly less stabilized than malonate (*e.g.* an enolate). In contrast, strong alkyl donors (with a σ-hybrid energy of −12 eV) seem theoretically more inclined toward the attack at the C_c atom but end up attacking the metal atom itself. In this case, the new governing factors of the reactivity remain to be explored.

In Figure 3, we present a Walsh diagram relative to the overall pathway of the reaction leading to metallacyclobutane. All of the five parameters, defined in **VI** and **IX**, are synchronously varied. The energy of the H_{1s} orbital, used as the nucleophile, is artificially fixed at −12.5 eV. The diagram features the low-lying C_3-$\pi_\perp$ MO that, in spite of the destabilizing loss of parallelism between the carbon p_π orbitals, is soon stabilized by the bonding interaction with Nu. Eventually, the level becomes a localized C_c–Nu bonding MO. Analogously, the well-known LUMO of the $(\eta^3$-allyl)M complex (C_3-$\pi_\perp$*), after the initial stabilization, *feels* the presence of the nucleophile and starts to convert into the very high lying C–H σ* level.

The character of the six intermediate filled MO's can be monitored. Interestingly, the bonding interaction [d_π-nC_3] (see the antibonding partner in **IV**) is not very much affected by the geometrical rearrangement and its energy remains almost constant. When the nucleophile is still far away, its σ hybrid falls almost at the same energy as the four metal nonbonding d orbitals (local square-planar environment). However, even in the early stages of the pathway, this accidental degeneracy forces important mixings between some of the levels having equal symmetry. At the metallacyclobutane structure, four nonbonding d orbitals are again easily individualized (the metal is still coordinated in a square-planar fashion), whereas the HOMO has deeply changed through a series of mixings and *avoided crossings*. As shown in **XII**, the HOMO is an overall bonding combination for the four-membered MC_3 ring. It is interesting to understand how the new character is acquired.

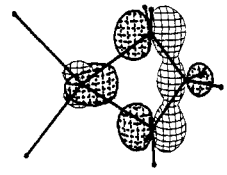

XII

Initially, the HOMO is an almost pure, nonbonding z^2-type metal orbital. Soon, it mixes in the character of the out-of-phase (antibonding) combination between C_3-$\pi_\perp$ and H_{1s} (the quickly rising MO that causes the four-electron repulsion). At some point, the descending LUMO and the rising HOMO undergo an *avoided crossing* (dotted lines). Through the latter, the levels mix into each other and, in particular, the mixing of the original C_3-$\pi_\perp$ and C_3-$\pi_\perp$* characters almost cancels any contribution of the C_c $\pi_\perp$ atomic orbital from the HOMO. For this reason, the level in question remains energetically constant while it smoothly transforms into the MC_3 σ-bonding combination **XII**. In contrast, the LUMO becomes centered first at the C_c atom and evolves later into the σ*(C_c-Nu) MO, which destabilizes quickly.

The *avoided crossing* allows two electrons to change their function. From populating an initial σ*(C_c-Nu) level, source of the barrier, they become smoothly bonding for the MC_3 cycle. From another viewpoint, the two electrons, which eventually localize at the C_t atoms, are formally donated to the metal.

In summary, the features of the diagram suggest that two electron pairs, from the nucleophile and from a π-bonding combination of C_3H_5 (C_3-$\pi_\perp$), win the initial repulsion because one of them concentrates in an in-phase combination of σ orbitals at the C_t atoms and the other one ends up forming the new C_c–H bond.

Conclusions

Although for a long time the attack of a nucleophile at a $(\eta^3$-allyl)M complex has been almost exclusively thought

(23) A detailed description of the relative pathway will be published in due course.

to lead to olefin products, the examples of nucleophilic attack at the central carbon atom are now numerous.[3,8] This type of reactivity seemed precluded for $[(\eta^3\text{-allyl})ML_2]^+$ species (M = Pd, Pt), but it is now shown to lead to platinacyclobutane complexes upon a proper selection of the nucleophile. The proposed MO mode, far from being exhaustive, highlights some important electronic aspects. First, it is shown that the discriminants for the attack at the C_c or C_t atoms are very subtle, or better perhaps, the regioselectivity is almost ambivalent.[8] For this reasons, only a direct exploration of the alternative reaction pathways and the dynamics of the MO pictures can properly settle the problem.

Although $[(\eta^3\text{-allyl})ML_2]^+$ models contain only a relatively low number of atoms, the application of sophisticated computational methods is problematic, as the structural rearrangements in the least-motion pathways of the nucleophilic attack are not trivial. The flexibility of the semiempirical packages is still best suited to picture the dynamics of the MO system and, hence, to detect basic trends. We have pointed out the following.

The pathway toward metallacyclobutane is characterized by an energy barrier whose origin is clearly attributable to a four-electron repulsion between the nucleophile and the C_c atom in the early part of the reaction. The extent of the barrier depends on the relative σ-donor strength of the nucleophile. The stronger the nucleophile, the smaller the barrier. However, very strong nucleophiles (such as methyl anions) which apparently eliminate the barrier, prefer to direct their attack to the metal. The prevailing electronic factors, in this case, remain to be explored. Also, the formation of metal–olefin adducts (a detailed analysis is to be reported elsewhere) seems unaffected by the type of four-electron repulsion that is so critical in the pathway to metallacyclobutanes.

As a very final conclusion, the attack at the C_c atom of $[(\eta^3\text{-allyl})M]^+$ complexes seems a more difficult event than that at any C_t atom but, for a proper combination of nucleophile and metal substrate, it can definitely be carried out. In this latter case, the implication that the energy barrier is strongly reduced or minimized seems to be consistent with the earlier observation[3] that the reaction is kinetically controlled even in spite of a possibly unfavorable thermodynamics of the products.

Experimental Section

NMR spectra were recorded on a Brüker AC-200 instrument and assigned by 2D and NOE experiments. IR spectra were recorded on Nujol mulls with a Brüker FT-48 instrument. GC analyses were performed with a DANI 3800 instrument equipped with a 0.25 mm × 30 m capillary column coated with SE 30 or with a 2 mm × 2 m glass column packed with 5% Carbowax on Chromosorb W-DMCS.

Materials. The ligands were Fluka products and were used as received. Ketene silyl acetals,[24] ketone silyl enolates,[25] $((allyl)PtCl)_4$,[10] and $C_2H_4Pt(PPh_3)_2$[26] were prepared according to published procedures. All the preparations were carried out under nitrogen purified by passage through R3-11 BASF catalyst. Workup of the reaction mixtures was performed in the air. Two standard methods were followed for the reaction of allyl–Pt acetate complexes and silyl ketene acetals according to the Pt source, respectively $(allylPtCl)_4$ (method A) and $C_2H_4Pt(PPh_3)_2$ (method B). One example will be reported for each preparation method.

Method A. Bis(tricyclohexylphosphine)-3-(1-carbomethoxy-1-methylethyl)platina(II)cyclobutane (4a). $P(C_6H_{11})_3$ (0.125 g, 0.56 mmol) dissolved in methylene chloride (3 mL) was added to $((allyl)PtCl)_4$ (0.076 g, 0.07 mmol) suspended in methylene chloride (7 mL). The mixture was stirred for 0.5 h to yield a colorless solution. TlOAc (0.085 g, 0.32 mmol) was then added, followed by 1-methyl-2-methoxy-2-(trimethylsiloxy)-propene (1, R = CH_3; 0.195 g, 1.12 mmol). The reaction mixture was stirred for 3 h and then centrifuged to eliminate TlCl. Evaporation of CH_2Cl_2 yielded a semisolid white residue, which was triturated with methanol to yield **4a** (0.150 g, 60% yield) as a white microcrystalline material pure by NMR control. Occasionally a small impurity was observed in the ^{31}P NMR spectrum (δ 19.07, $CDCl_3$). An analytically pure sample was obtained by crystallizing from CH_2Cl_2/hexane. Anal. Calcd for $C_{44}H_{80}O_2P_2Pt$: C, 58.84; H, 8.98. Found: C, 58.94; H, 8.93. IR: ν_{CO} 1724 cm^{-1}.

Method B. Bis(triphenylphosphine)-3-methyl-3-(1-carbomethoxy-1-methylethyl)platina(II)cyclobutane (6a). Methallyl acetate (0.159 g, 1.4 mmol) was added to a methylene chloride solution (3 mL) of $C_2H_4Pt(PPh_3)_2$ (0.26 g, 0.35 mmol). The mixture was stirred for 15 min, and then 1-methyl-2-methoxy-2-(trimethylsiloxy)propene (1, R = Me; 0.487 g, 1.4 mmol) was added. The resulting solution was kept at room temperature for 3 h. The solvent was then evaporated and the residue triturated with methanol to yield **6a** (0.248 g, 81% yield) as a white microcrystalline material pure by ^{31}P NMR control. An analytically pure sample may be obtained by crystallizing from CH_2Cl_2/hexane. Anal. Calcd for $C_{45}H_{46}O_2P_2Pt$: C, 61.70; H, 5.30. Found: C, 61.42; H, 5.17. IR: ν_{CO} 1713 cm^{-1}.

Bis(triphenylphosphine)-3-(1-carbomethoxy-1-methylethyl)platina(II)cyclobutane (4b): method A; 61% yield. Anal. Calcd for $C_{44}H_{44}O_2P_2Pt$: C, 61.3; H, 5.1. Found: C, 61.32; H, 5.50. IR: ν_{CO} 1717 cm^{-1}.

(1,4-Bis(diphenylphosphino)butane)-3-(1-carbomethoxy-1-methylethyl)platina(II)cyclobutane (4c): method A; 45% yield. Anal. Calcd for $C_{36}H_{42}O_2P_2Pt$: C, 56.67; H, 5.5. Found: C, 56.06; H, 5.38. IR: ν_{CO} 1720 cm^{-1}.

(1,4-Bis(diphenylphosphino)butane)-3-(1-carbomethoxyethyl)platina(II)cyclobutane (4d): method A; 47% yield. Anal. Calcd for $C_{35}H_{40}O_2P_2Pt$: C, 56.07; H, 5.38. Found: C, 55.94; H, 5.29. IR: ν_{CO} 1724 cm^{-1}.

(1,2-Bis(diphenylphosphino)ethane)-3-(1-carbomethoxy-1-methylethyl)platina(II)cyclobutane (4e): method A; 43% yield. Anal. Calcd for $C_{34}H_{38}O_2P_2Pt$: C, 55.5; H, 5.21. Found: C, 54.65; H, 5.09. IR: ν_{CO} 1720 cm^{-1}.

Bis(triphenylphosphine)-3-methyl-3-(1-carbomethoxyethyl)platina(II)cyclobutane (6b): method B; 48% yield. Anal. Calcd for $C_{44}H_{44}O_2P_2Pt$: C, 61.30; H, 5.11. Found: C, 61.42; H, 5.16. IR: ν_{CO} 1717 cm^{-1}.

Bis(triphenylphosphine)-2-methyl-3-(1-carbomethoxy-1-methylethyl)platina(II)cyclobutane (6c/6e, 3:1): method B; 65% yield. Anal. Calcd for $C_{45}H_{46}O_2P_2Pt$: C, 61.70; H, 5.30. Found: C, 61.56; H, 5.17. IR: ν_{CO} 1715 cm^{-1}.

Bis(triphenylphosphine)-2,4-dimethyl-3-(1-carbomethoxy-1-methylethyl)platina(II)cyclobutane (6d/6f, 4:1): method B; 73% yield. Anal. Calcd for $C_{46}H_{48}O_2P_2Pt$: C, 62.07; H, 5.44. Found: C, 61.87; H, 5.36. IR: ν_{CO} 1720 cm^{-1}.

Bis(triphenylphosphine)-3-(1-methyl-2-oxobutyl)platina-(II)cyclobutane (8). PPh_3 (0.104 g, 0.4 mmol) was added to a suspension of $((allyl)PtCl)_4$ (0.054 g, 0.05 mmol) in CH_2Cl_2 (7 mL) to yield a pale yellow solution. After addition of (*Z*)-2-(3-trimethylsiloxy)pentene (0.063 g, 0.4 mmol) the mixture was cooled to −80 °C. A CH_2Cl_2 (3 mL) solution of $[NBu_4]^+F^-$ (0.120 g, 0.4 mmol) was slowly added. The mixture was allowed to reach room temperature within 4 h. The solvent was then evaporated and the residue triturated with methanol to yield 8 as an off-white solid (0.073 g, 43% yield). Analytically pure samples were obtained by stratifying a methylene chloride

(24) (a) Ainsworth, C.; Chen, F.; Yu-Neng, K. J. *J. Organomet. Chem.* **1972**, *46*, 59. (b) Ireland, R. E.; Muller, R. H.; Willard, A. K. *J. Am. Chem. Soc.* **1976**, *98*, 2868.

(25) Cazeau, P.; Duboudin, F.; Moulines, F.; Babot, O.; Dunogues, J. *Tetrahedron* **1987**, *43*, 2075.

(26) Nagel, U. *Chem. Ber.* **1982**, *115*, 1988.

solution of 8 with hexane. Anal. Calcd for $C_{44}H_{44}OP_2Pt$: C, 62.47; H, 5.25. Found: C, 62.09; H, 5.40. IR: ν_{CO} 1697 cm^{-1}.

Bis(triphenylphosphine)-3-(2-oxocyclopentyl)platina-(II)cyclobutane (10) was prepared similarly to 8 in 44% yield. Anal. Calcd for $C_{44}H_{42}OP_2Pt$: C, 62.63; H, 5.02. Found: C, 62.75; H, 5.17. IR: ν_{CO} 1724 cm^{-1}.

Computational Details. All the MO calculations were of the extended Hückel type, and a modified version of the Wolfsberg–Helmholz formula was used. The atomic parameters used for the main elements, including the metals Pd and Pt, are taken from refs 27 and 28, respectively. Other geometric details (beside those already specified in the text) are as follows: M–P distances, 2.25 Å; M–C_c and M–C_t distances in the (η^3-allyl)M-$(PH_3)_2$ model, 2.05 Å (M = Pd, Pt); C_t–C_c–C_t angle, 120°. The graphics presented in the paper, including three-dimensional MO drawings, have been obtained by using the program CACAO.[29]

Acknowledgment. This research has been supported by the Progetto Finalizzato CNR, Chimica Fine II, and the MURST. The work of K.L. and J.A.L., c/o ISSECC, has been made possible through grants from the Commission of the European Communities and the Ministerio de Educación y Ciencia of the Spanish Government, respectively.

OM9300179

(27) Tatsumi, K.; Hoffmann, R.; Yamamoto, A.; Stille, J. K. *Bull. Chem. Soc. Jpn.* **1981**, *54*, 1857.
(28) Summerville, R. H.; Hoffmann, R. *J. Am. Chem. Soc.* **1976**, *98*, 7240.
(29) Mealli, C.; Proserpio, D. M. *J. Chem. Educ.* **1990**, *67*, 399.